Biochimica et Biophysica Acta 893 (1987) 138–148
Elsevier

BBA 42578

Light-induced oxidation of the acceptor-side Fe(II) of Photosystem II by exogenous quinones acting through the Q_B binding site. II. Blockage by inhibitors and their effects on the Fe(III) EPR spectra

Bruce A. Diner [a] and Vasili Petrouleas [b]

[a] *Institut de Biologie Physico-Chimique, Paris (France) and* [b] *Nuclear Research Center 'Demokritos', Athens (Greece)*

(Received 7 November 1986)
(Revised manuscript received 7 May 1987)

Key words: Electron spin resonance; Photosystem II; Quinone-iron acceptor complex; Fe(III); Reduction-induced oxidation; Herbicide inhibitor

Four representative inhibitors of Photosystem II (PS II) Q_A^- to Q_B electron transfer were shown to bind, at high concentrations, to PS II reaction centers having the acceptor-side non-heme iron in the Fe(III) state. Three of the inhibitors studied, DCMU, *o*-phenanthroline and dinoseb, modified the EPR spectrum of the Fe(III) relative to that obtained by ferricyanide oxidation in the absence of inhibitor. *o*-Phenanthroline gave particularly axial symmetry, while DCMU and dinoseb gave more rhombic configurations. The herbicide inhibitor, atrazine and its analogue, terbutryn, had no effect. The dissociation constants for inhibitor binding to reaction centers in the Fe(III) state were measured directly and also estimated from shifts in the midpoint potential of the Fe(III)/Fe(II) couple and were shown to increase by factors of approx. 100, approx. 10 and 10–15 for DCMU (pH 7.5), atrazine (pH 7.0) and *o*-phenanthroline (pH 7.0), respectively, upon oxidation of the iron. Atrazine and *o*-phenanthroline, which induce the smallest changes in the midpoint potential of the Fe(III)/Fe(II) couple, were shown to inhibit light-induced oxidation of the Fe(II) by phenyl-*p*-BQ, described in the preceding paper (Petrouleas, V. and Diner, B.A. (1987) Biochim. Biophys. Acta 893, 126–137). The extent of inhibition was much greater than would be predicted from a simple shift in the midpoint potential for Fe(III)/Fe(II) and we conclude that phenyl-*p*-BQ and the other quinones, which show light-induced oxidation, act through the Q_B binding site. It is also argued that reduction and oxidation of the iron by ferro- and ferricyanide, respectively, occur through this site. The effects of these inhibitors and of various quinones on the Fe(III) environment are discussed with reference to the known contact points between the protein and *o*-phenanthroline and terbutryn in the Q_B binding pocket of *Rhodopseudomonas viridis* reaction centers (Michel, H., Epp, O. and Deisenhofer, J. (1986) EMBO J. 5, 2445–2451). The Fe(III) EPR spectrum is thus a new and sensitive probe of the contact points at which molecules bind to the Q_B binding site.

Abbreviations: BBY, Berthold, Babcock and Yocum (see Ref. 25); DCMU, diuron (3-(3,4-dichlorophenyl)-1,1-dimethylurea); EDTA, ethylenediaminetetraacetate; EPR, electron paramagnetic resonance; F, fluorescence yield; F_0, Photosystem II fluorescence yield with Q_A oxidized; Hepes, 4-(2-hydroxyethyl)-1-piperazineethanesulfonic acid; Mes, 4-morpholineethanesulfonic acid; *p*-BQ, 1,4-benzoquinone; PQ-9, plastoquinone *a*; PS II, Photosystem II; RC, reaction center; Q_A, primary quinone electron acceptor; Q_B, secondary quinone electron acceptor; Q_{ex}, exogenous quinone.

Correspondence: B.A. Diner, (present address:) Central Research and Development Department, Experimental Station E402/2224, E.I. du Pont de Nemours & Co. Inc., Wilmington, DE 19898, U.S.A.

Introduction

There has been considerable interest in recent years in understanding how herbicide inhibitors block electron transfer between the primary and secondary quinone acceptors, Q_A and Q_B, respectively, of reaction centers of Photosystem II (PS II) and those of purple photosynthetic bacteria [1–6] (for a review, see Ref. 7). Attention of biophysicists has focused principally on four classes of inhibitors: the ureas, the triazines, the phenolics and *o*-phenanthroline. These have been shown to compete with quinone for binding to the reaction center [1–7]. The site of binding has, in a number of cases, been determined by photoaffinity labelling [8–13]. Isolation of herbicide-resistant mutants has provided clues as to the region of the D1 polypeptide of the PS II reaction center [14–16] and of the L subunit of the bacterial reaction centers [12,17] to which these inhibitors bind and with what amino acid residues they interact. More recently, the determination of the X-ray crystallographic structure of *Rps. viridis* reaction centers to better than 3 Å resolution [18] has shown the inhibitor binding site to be located within the L subunit, in agreement with earlier photoaffinity labelling studies [11,12], and has indicated the amino acid residues within this site which interact with *o*-phenanthroline and terbutryn to assure their binding. That the inhibitor binding site is also that for Q_B, is indicated by recent crystallographic data on *Rhodobacter sphaeroides* reaction centers [19,20].

In this paper we describe a new probe for the detection of herbicide binding in the Q_B pocket of the PS II reaction center. The acceptor-side iron of the reaction center can be oxidized to Fe(III) [21], and can function in this state as the high-potential electron acceptor to Q_A^-, Q_{400} [22,23]. The low-field X-band EPR signals one detects for Fe(III) are highly sensitive to the nature of the molecules bound to the Q_B binding site. Different herbicides (this paper) as well as exogenous quinones (accompanying paper: Ref. 24) induce different ligand field symmetries at the iron site which are revealed in the EPR spectra. The inhibitors also modify the midpoint potential of the Fe(III)/Fe(II) redox couple, an observation which is consistent with an earlier finding of Wraight [25] of a decrease in binding affinity of herbicide inhibitors upon oxidation of Q_{400}. We will show that the binding of herbicides to the Q_B-binding site blocks the light-induced oxidation of the iron by exogenous quinones [24,26] demonstrating that such oxidation occurs through the Q_B binding site.

Materials and Methods

Photosynthetic membranes. Thylakoid membrane fragments (BBY membranes [27]) were prepared and used as described in the preceding paper [24]. All inhibitors and exogenous quinones were added from stock solutions in DMSO. The quinone concentration was typically 0.5 to 1 mM and the DMSO concentration never exceeded 0.5% (v/v). An equivalent concentration of DMSO was added to all control samples.

Electron spin resonance spectroscopy. The electron spin resonance spectrometer and cryostat were as described previously [21]. The EPR detection conditions were as described in the Material and Methods section of the preceding paper [24].

Fluorescence relaxation kinetics. The fluorescence relaxation kinetics were determined following saturating microsecond actinic flash excitation with broad band blue light (Schott BG 39). The fluorescence yield was probed by 492 nm microsecond detecting flashes at various times following the actinic flash. The instrument used was the flash detection spectrophotometer of the preceding paper [24].

Results

Influence of inhibitors on the Fe(III) EPR spectra

BBY membranes at pH 7.0 were incubated with 5 mM ferricyanide to oxidize the PS II acceptor-side Fe(II) to Fe(III). The membranes were then incubated at 0 °C with atrazine, DCMU, *o*-phenanthroline and dinoseb or with no further additions. The EPR spectra are shown in Fig. 1 (continuous lines). The background spectra, recorded after saturating illumination at 200 K are shown as dotted traces. The spectra for those samples containing ferricyanide alone are shown at the upper left of Fig. 1 (see also Figs. 3 and 6). These spectra, containing only two resonances at $g = 8$ and $g = 5.5$, are simpler than earlier ones

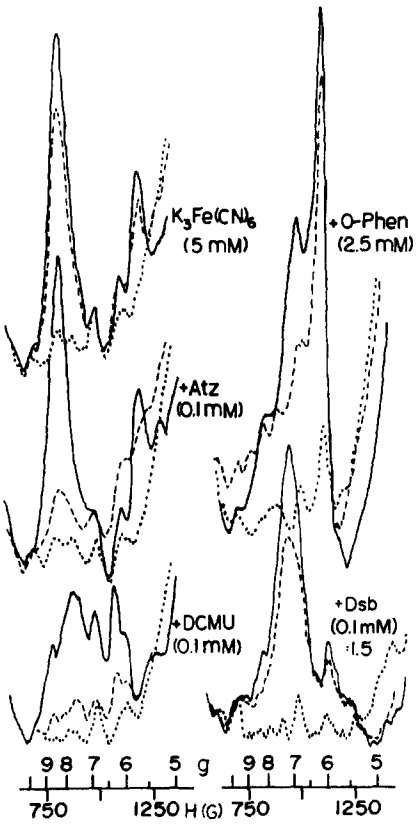

Fig. 1. Effect of inhibitors on the shape of the Fe(III) EPR signals. BBY membranes at pH 7 were incubated for 50 min at 0 °C with 5 mM $K_3Fe(CN)_6$ (E_h = 490–495 mV). Atrazine (Atz), DCMU, *o*-phenanthroline (O-phen) and dinoseb (Dsb) were added at the indicated concentrations and incubated for an additional 2 h 30 min at 0 °C, after which the continuous line spectra were recorded. The samples were illuminated at 200 K (dotted lines) and then dark-adapted at 0 °C for an additional 2 h (dashed lines). The EPR spectra in this figure and in the following figures were recorded under the conditions described in the Materials and Methods section of the accompanying paper [24].

taken on mutants of *Chlamydomonas* [21], which contained an additional resonance at $g = 6.4$. A preliminary study of the $g = 8$ and $g = 5.5$ resonances indicated a similar temperature dependence for the two. We cannot tell if the $g = 5.5$ signal is derivative or peak shaped because of the close proximity of the $g = 4.3$ impurity resonance. Whether the $g = 8$ and $g = 5.5$ signals arise from the same spin multiplet or from centers with different local distortions is therefore not yet clear. It should also be noted that spectra, similar to those in BBY preparations, can also be observed in spinach chloroplasts in the presence of ferricyanide at pH 7.5 (not shown).

A comparison of the Fe(III) signals following addition of the various herbicides (Fig. 1) shows that 0.1 mM atrazine does not alter the Fe(III) spectrum with respect to that obtained with ferricyanide alone. The same is true for 0.1 mM terbutryn (not shown). DCMU, *o*-phenanthroline and dinoseb (Fig. 1) distort significantly the lineshape. The DCMU spectrum consists of a series of signals between $g = 6$ and $g = 8$, indicating that binding of this inhibitor induces various local rhombic distortions at the iron site in different reaction centers. The spectrum in the presence of 2.5 mM *o*-phenanthroline consists of a sharp, nearly axial $g = 6$ component and weaker contributions between $g = 6$ and $g = 8$. High concentrations and/or long incubation times increase the relative size of the axial contribution (see Fig. 2). Dinoseb (0.1 mM) induces a $g = 7$ peak and weaker contributions at $g = 6$ and $g = 5.5$; additional peaks at *g*-values intermediate between 6 and 7 and of varying size (stronger at higher concentrations) were also observed in different preparations. After 2 h of dark incubation, following illumination at 200 K (Fig. 1, dashed line), about 25% of the signal with ferricyanide alone is restored in the presence of 0.1 mM DCMU, 35% with 0.1 mM atrazine, 90–100% with 2.5 mM *o*-phenanthroline, and 85% with 0.1 mM dinoseb.

Effect of inhibitors on the midpoint potential of Fe(III)/Fe(II)

The experiments of Fig. 1 indicate that atrazine and DCMU, and to a smaller extent, dinoseb and *o*-phenanthroline either prevent access of ferricyanide to the Fe(II) (kinetic limitation of oxidation) or elevate the midpoint potential of the Fe(III)/Fe(II) couple (thermodynamic limitation) or both at the same time.

Two methods were used to estimate the inhibitor-induced displacement of the midpoint potential of the Fe(III)/Fe(II) couple. The first and more accurate arises from the dependence of the midpoint potential on the inhibitor dissociation constants for reaction centers in the Fe(III) and Fe(II) forms. The second involved measurement of the extent of oxidation of the iron at a given

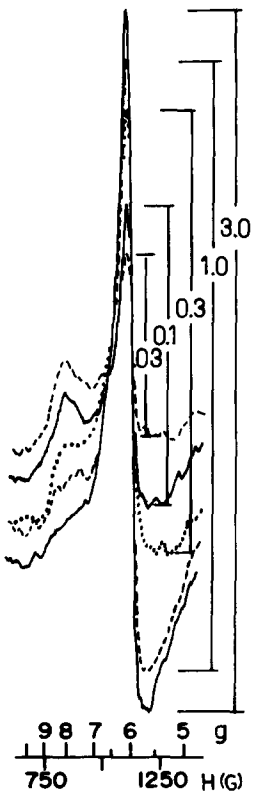

Fig. 2. Effect of increasing concentrations of *o*-phenanthroline on the EPR spectrum of Fe(III). BBY membranes (2.5 mg Chl/ml in 15 mM Hepes, pH 7.0) were incubated with 5 mM $K_3Fe(CN)_6$ for 50 min and then incubated for an additional 80 min in the presence of the indicated *o*-phenanthroline concentrations. The spectra were displaced for reasons of clarity. The EPR spectra obtained, following illumination of these samples at 200 K, were practically featureless.

potential and inhibitor concentration and amounted to a check of the first method.

The following equation relates the midpoint potential for the E_m of Fe(III)/Fe(II) in the presence of the inhibitor to that in its absence:

$$E_m(\text{Fe(III)}_i/\text{Fe(II)}_i) = E_m(\text{Fe(III)/Fe(II)}) + 59 \log \frac{1 + I/K_2}{1 + I/K_3} \quad (1)$$

where I = inhibitor concentration, K_2 is the inhibitor dissociation constant for Fe(II) reaction centers RC-Fe(II) (I) = RC-Fe(II) + I, and K_3 is the inhibitor dissociation constant for Fe(III) reaction centers RC-Fe(III) (I) = RC-Fe(II) + I.

The dissociation constant, K_2, was estimated from a titration of the rate of reoxidation of Q_A^- as a function of inhibitor concentration in Fe(II) centers, BBY membranes were suspended at 10 μg Chl/ml in 50 mM Hepes, 5 mM $MgCl_2$, 15 mM NaCl, 3 mM EDTA and 0.4 M sucrose. The pH was 7.0 for atrazine and *o*-phenanthroline and 7.5 for DCMU. The inhibitors were added in DMSO, whose concentration never exceeded 0.3%. Photosystem II was excited by a saturating microsecond actinic flash and the fluorescence relaxation followed in the flash detection spectrophotometer from 500 μs onward. The fluorescence yield ratio, $(F_{200\,ms} - F_0)/(F_{500\,\mu s} - F_0)$ (0.3 in uninhibited centers), was used as an indicator of the fraction of centers having a bound inhibitor. F_0 is the fluorescence yield with Q_A oxidized. This ratio, which was taken as a linear indicator of the per-

TABLE I

SUMMARY OF DISSOCIATION CONSTANTS, K_2 AND K_3, OF INHIBITORS FOR REACTION CENTERS IN THE Fe(II) AND Fe(III) STATES, RESPECTIVELY

Also shown is the ratio of K_3 to K_2 estimated from the figures of Ref. 25 for centers in the Q^+_{400} and Q_{400} states, respectively. The E_m were calculated from the K_2 and K_3 measured directly (column 4) and from the data of Figs. 3 and 4 (column 5). The ΔE_m values of column 5 are measured indirectly and are subject to greater error than those of column 4. The values of column 4 are more accurate as they involve direct determination of the dissociation constants.

Inhibitor	K_2	K_3	ΔE_m from Eqn. 1 for K_3/K_2 ($[I]_{sat}$)	ΔE_m from Figs. 3 and 4	K_3/K_2 from Ref. 25
Atrazine (pH 7)	210 nM	≤ 2–3 μM	≤ 60 mV	≈ 65 mV	1
DCMU (pH 7.5)	80 nM	5–10 μM	≈ 120 mV	≈ 120 mV	300
o-Phenanthroline (pH 7)	9 μM	140 μM	65–70 mV	20–25 mV	5

cent of inhibited centers, ranged from 0.3 for uninhibited centers to 0.80–0.85 for fully inhibited centers. The concentration of inhibitor (atrazine, DCMU and *o*-phenanthroline) which blocked half the centers was taken as K_2. The results of these titrations are shown in Table I.

K_3 was measured in the EPR as the concentration necessary to transform, in one-half the centers, the Fe(III) EPR spectrum from that observed with 5 mM ferricyanide alone to that observed for the various inhibitors in Fig. 1. An example of such a titration is indicated in Fig. 2 for *o*-phenanthroline, the most accurate because of its elevated K_3. These experiments were done at 1.5–3 μM PS II reaction centers to minimize depletion of added inhibitor by specific and non-specific binding. For atrazine, which is the most difficult to measure, the dissociation constant was determined by the ability of this inhibitor to displace 4 mM *p*-BQ from the reaction center (see Fig. 6). The results for K_3 are also given in Table I.

K_3 was also estimated by the decrease in the amplitude of the Fe(III) EPR signals upon addition of inhibitor at known potentials (E_h). BBY membranes (Fig. 3) were first incubated at two concentrations of ferri- + ferrocyanide differing by a factor of 4 but with the same final ratio of ferri-/ferrocyanide ($E_h = 465$ mV). They were then incubated with 30 μM DCMU for 2 h at 0 °C. The Fe(III) EPR spectra were recorded (continuous lines) and the membranes illuminated at 200 K to return to Fe(II) (dotted spectra). They were then incubated for an additional 2 h in darkness and the regenerated Fe(III) signals were again recorded (dashed lines). At the higher concentrations of oxidant and reductant (Fig. 3, lower right) the initial and regenerated Fe(III) signals are the same amplitude as they are at both concentrations in the absence of inhibitor (Fig. 3, left), indicating full equilibration of the iron with the ferri- and ferrocyanide. The amplitude of the signal obtained is about 25% of that obtained in Fig. 1 in the presence of DCMU at high ambient potential ($E_h = 490$–495). With an E_m of 370 mV for Fe(III)/Fe(II) at pH 7.5 and an ambient redox potential, E_h, of 465 mV (Fig. 3), this decrease in signal amplitude implies an increase in E_m for Fe(III)/Fe(II) of approx. 120 mV, in approximate agreement with the ratio of 100 for K_3/K_2 for this inhibitor (Table I).

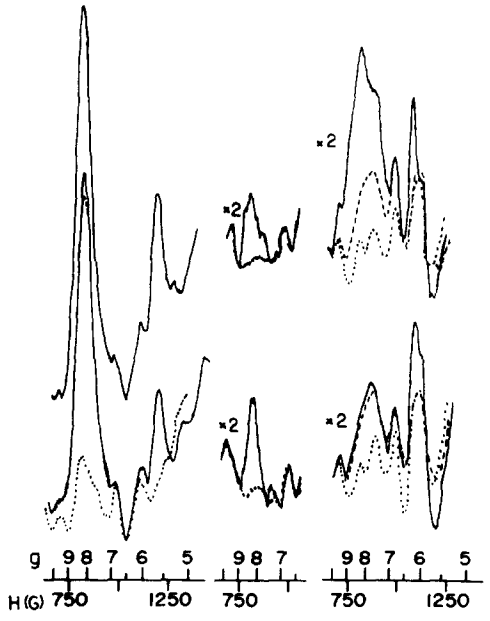

Fig. 3. Effect of ferri- and ferrocyanide concentrations on the rate of redox equilibration of the PS II acceptor-side iron in the presence of 30 μM DCMU. BBY membranes (pH 7.5) were incubated for 1 h at 0 °C with ferri-/ferrocyanide at 5.6 mM/1.9 mM (upper) or 22 mM/7.3 mM) (lower), respectively. The E_h was 465 mV in both cases. The samples were then incubated for an additional 2 h at 0 °C following addition of 30 μM DCMU (right, continuous line spectra) or after lowering the pH to 5.2 with 100 mM Mes (middle, continuous line spectra). The control samples on the left were incubated for the same length of time with no further additions (continuous line spectra). The spectra were recorded again after illumination at 200 K (dotted line) and after further dark adaptation for 2 h at 0 °C (dashed line). Dotted and dashed-line traces are not shown in the upper left spectrum for reasons of clarity.

The experiments of Fig. 3 indicate that, in the absence of DCMU, the iron equilibrates with ferri- and ferrocyanide at both sets of concentrations and for both types of perturbations – either light-driven reduction of the Fe(III) (left) or a pH drop from 7.5 to 5.2 (center) which raises the midpoint potential of the iron by approx. 140 mV (−60 mV/pH unit [21]). That at the lower set of ferri- and ferrocyanide concentrations the level of Fe(III) attained after illumination remains below that preceding illumination (upper right) implies that DCMU slows the rate of interaction of ferrocyanide with the iron.

The possibility that the difference in ionic strength may have influenced the reaction rate of ferri-/ferrocyanide was also tested (data not shown). A mixture of ferri-/ferrocyanide (1.5 mM/0.25 mM, respectively) was added to BBY membranes in the presence of 30 μM DCMU and the Fe(III) EPR spectrum recorded after 2 h incubation. In a parallel experiment, addition of 45 mM KCl did not modify the final amplitude of Fe(III).

To verify the binding affinities of atrazine and *o*-phenanthroline, BBY membranes were first incubated with ferri-/ferrocyanide ($E_h \approx 465$ mV) followed by addition of 30 μM atrazine or 2.5 mM *o*-phenanthroline or treated in the reverse order: inhibitor first and then the same concentration and ratio of mediators (Fig. 4). The signal amplitudes were nearly the same irrespective of the order of addition. That equilibrium was attained, despite the use of lower ferri- plus ferrocyanide concentration than in Fig. 3, implies that atrazine and *o*-phenanthroline have a higher rate of turnover than does DCMU. This observation is consistent with the results of Vermaas et al. [29].

Addition of 30 μM atrazine (Fig. 4) lowers the $g = 8$ signal amplitude by approx. 50%. With an $E_{m,7}$ of 400 mV for Fe(III)/Fe(II) and an E_h of 465 mV, this decrease corresponds to a positive shift in the E_m of about 65 mV ($K_3/K_2 \approx 14$), again in approximate agreement with the upper limit set for the K_3 for atrazine.

For *o*-phenanthroline the change in midpoint potential is somewhat more difficult to estimate because of the radical change in the Fe(III) signal shape. Nonetheless, one can compare the signal amplitude at $g = 6$ in Fig. 1 (with *o*-phenanthroline) and the $g = 8$ in the same figure (without *o*-phenanthroline, $E_h = 495$ mV) with those analogous features in Fig. 4, where $E_h = 465$ mV. At the higher potential of Fig. 1, there is practically no reduction upon addition of any of the inhibitors. At $E_h = 465$ mV (Fig. 4) the loss in $g = 6$ signal amplitude is approx. 20% after normalization to the $g = 8$ signal or an increase in the $E_{m,7}$ of about 20–25 mV. The direct determination of K_2 and K_3 is, however, much more reliable for this inhibitor as each is well above the concentration of reaction centers. Fig. 4 also shows that the transition of the Fe(III) EPR spectrum from $g = 8$ to $g = 6$ upon addition of *o*-phenanthroline is not immediate and occurs on the minutes time scale.

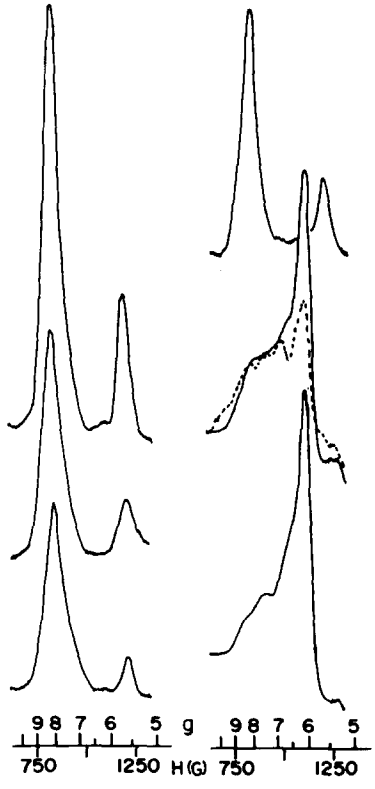

Fig. 4. Effect of 30 μM atrazine (left) and of 2.5 mM *o*-phenanthroline (right) on the Fe(III) signal amplitudes in the presence of ferri-/ferrocyanide (2.6 mM/0.7 mM, respectively, pH 7.0). The upper curves were recorded after incubation for 3 h at 0 °C with ferri-/ferrocyanide alone. The middle set of spectra were recorded after incubation for 1 h with ferri-/ferrocyanide and then for 2 h with inhibitor (0 °C). The dashed trace was recorded less than 1 min after addition of *o*-phenanthroline. The lower set of spectra were recorded after 20–30 min incubation with inhibitor, followed by a 3 h incubation with ferri-/ferrocyanide (0 °C). The light-insensitive background signals have been subtracted from these spectra.

Blockage by inhibitors of light-induced oxidation of Fe(II) by phenyl-p-BQ

The smaller shifts in midpoint potential of the Fe(III)/Fe(II) couple induced by *o*-phenanthroline and atrazine make these ideal inhibitors, then, to test for blockage of light-induced oxidation by exogenous quinones. These inhibitors are known to compete with quinone for binding to the reaction center [1–7,18,32,34] and a strong inhibition

of light-induced Fe(II) oxidation would imply that the exogenous quinones act through the Q_B site.

Fig. 5 shows that, in the presence of 1 mM phenyl-*p*-BQ, 2.5 mM *o*-phenanthroline or 30 μM atrazine decrease the formation of the light-induced Fe(III) to nearly 0 and 10%, respectively, of the control sample in the absence of inhibitor. The midpoint potential, $E_{m,7}$, of Q^-/QH_2 for phenyl-*p*-BQ was estimated in Table I of Ref. 24 to be 496 mV as calculated from literature values and some probable assumptions. A value of 455 mV provided the best fit for the pH-dependent behavior of the light-induced oxidation of the Fe(II) in the presence of phenyl-*p*-BQ (Fig. 7 of Ref. 24). Using both of these values for phenyl-*p*-BQ, the positive shift in $E_{m,7}$ for Fe(III)/Fe(II) by 2.5 mM *o*-phenanthroline and 30 μM atrazine of 60–65 mV should yield approx. 70 and approx. 40%, respectively, of Fe(II) oxidation as compared to the control. These calculations do not take into account competition between inhibitor and quinone for binding to the reaction center, a factor which would raise the estimated percent of iron oxidation. That, in both cases, the observed signals are much smaller than those predicted by positive displacement of the $E_{m,7}$ for Fe(III)/Fe(II) means that both inhibitors compete with phenyl-*p*-BQ for binding to the reaction center. That both inhibitors bind to the center is also seen (Fig. 5, right, dashed lines) by the long lived Q_A^-Fe(II) $g = 1.9$ signal observable following 200 K illumination and warming to 0 °C and totally absent in the control without inhibitor. In the latter case, Q_A^- has been oxidized by phenyl-*p*-BQ. With the inhibitors present (Fig. 4) the little reoxidation of Q_A^- that occurs (30%) does so presumably by back-reaction.

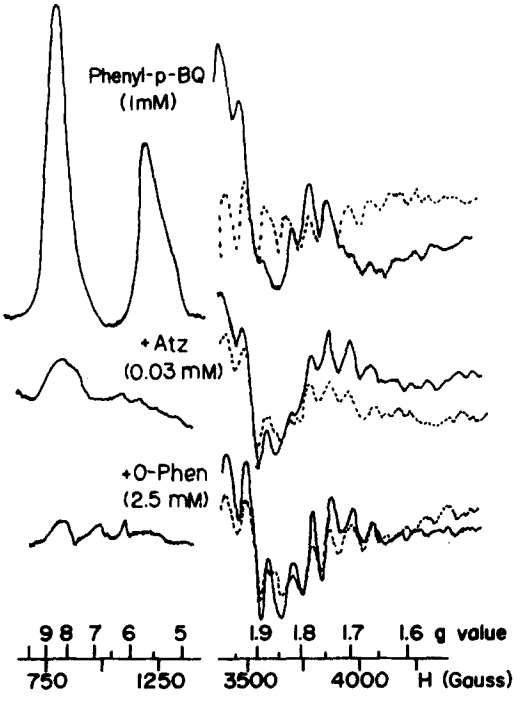

Fig. 5. Inhibition of light-induced Fe(III) formation in the presence of 1 mM phenyl-*p*-BQ by 30 μM atrazine (Atz) and 2.5 mM *o*-phenanthroline (O-phen). BBY membranes at pH 7.0 were illuminated at 200 K (continuous line spectra, right) and then warmed to 0 °C for 17 s in the dark (dashed line spectra, right). The continuous line spectra on the left are the difference spectra corresponding to dark 17 s incubation at 0 °C minus illumination at 200 K. Upper: control without inhibitor; middle: 30 μM atrazine; bottom: 2.5 mM *o*-phenanthroline.

Competition between atrazine and p-BQ for binding to the PS II reaction center

Additional evidence for competitive binding between atrazine and exogenous quinone is shown in Fig. 6. In this case BBY membranes were incubated at pH 7 with 5 mM $K_3Fe(CN)_6$ (E_h = 490–495 mV) to maximally oxidize the iron. The membranes were then incubated with 1 mM *p*-BQ alone or with 1 mM *p*-BQ plus 0.2 mM atrazine. In the former case, one sees (Fig. 6) the Fe(III) signals similar to those generated by light-induced oxidation in the presence of *p*-BQ (Fig. 5 of Ref. 24). The size of the $g = 8$ resonance decreased with increasing concentration of *p*-BQ (not shown) and verifying the assignment of $g = 6.8$ to centers having bound *p*-BQ. If atrazine is present, then the $g = 6.8$ peak is absent (Fig. 6, bottom) and the spectrum again resembles that of Fe(III) in the presence of atrazine alone (Fig. 1, middle, left). While we cannot absolutely exclude that atrazine imposes a particular configuration on the Fe(III) environment even with *p*-BQ present, the simpler and more likely interpretation is that atrazine displaces the *p*-BQ. This interpretation is all the more likely as atrazine blocks Q_A^- oxidation by exogenous quinones as we have already shown in Fig. 5.

Fig. 6. Displacement of reaction center-bound *p*-BQ by atrazine. BBY membranes at pH 7.0 were incubated with 5 mM $K_3Fe(CN)_6$ (E_h = 490–495 mV) for 50 min at 0 °C and then incubated for an additional 2 h in the presence of 1 mM *p*-BQ (middle) or 1 mM *p*-BQ plus 0.2 mM atrazine (Atz) (lower) or with no further additions (upper). The spectra shown are the differences between the spectra recorded before minus those recorded after illumination at 200 K.

Discussion

Michel et al. [18] have recently reported the crystallographic structure for *Rps. viridis* reaction centers containing either *o*-phenanthroline or terbutryn, both of which compete with ubiquinone for binding to the reaction center in photosynthetic bacteria [3,6]. This same site is now indicated to be that where ubiquinone, Q_B, binds in *Rb. sphaeroides* reaction centers. Michel et al. [18] show that *o*-phenanthroline binds with its two nitrogens sharing a H-bond with the imidazole nitrogen of histidine L190, coordinated to the Fe(II). Terbutryn, on the other hand, also binds to the Q_B binding site, but at some distance from the Fe(II), through H-bonds between one of the ring nitrogens and a peptide nitrogen of isoleucine L224, and a second H-bond between the ethylamine nitrogen and the hydroxyl group of serine L223. This binding site should also be the same for the structurally similar triazine, atrazine, which also binds to bacterial reaction centers [9,11–13, 28,30,31].

Deisenhofer et al. [33] and Trebst [34] have pointed out the strong homology between the D1 and D2 polypeptides of the PS II reaction center with the L and M subunits of the *Rps. viridis* reaction centers, particularly as regards the primary structure around the Fe-binding site. Thus, in PS II, it is probable that *o*-phenanthroline binds to one of the homologous iron-ligating histidines. Terbutryn and atrazine would more likely bind at a distance, but still within the Q_B site. These latter inhibitors would affect the Fe environment at best indirectly by displacement of the Q_B quinone or via an allosteric effect or shift of a pK of a coupled protonatable group. One of the latter two explanations is probably responsible for the shift in the $E_{m,7}$ for Fe(III)/Fe(II) upon binding of inhibitor.

The transformation of the Fe(III) site symmetry to axial (indicating most likely a greater equivalence of the histidine ligands), upon addition of *o*-phenanthroline to centers preincubated with ferricyanide alone, would be consistent with binding by this inhibitor to a site homologous to that in bacterial reaction centers. During the preparation of this manuscript, we learned of results from Itoh et al. [35] which agree with our findings concerning the EPR signal shape with *o*-phenanthroline and DCMU. At pH 7.5 we find, as do Itoh et al. [35] at pH 7.0, that DCMU induces mixed rhombic symmetry at the Fe(III) site. Itoh et al., point out, however, that at higher pH (8.7), the Fe(III) spectrum, in the presence of DCMU, becomes more axial, like that of *o*-phenanthroline. This observation would favor binding of DCMU to the same site as *o*-phenanthroline. That the binding sites are different for DCMU or *o*-phenanthroline on the one hand and the triazines on the other, is also supported by the varied differential sensitivity of herbicide-resistant *Chlamydomonas* mutants to DCMU and atrazine [15].

The absence of any change in line shape in the Fe(III) EPR spectrum between ferricyanide alone and ferricyanide plus atrazine would be consistent with atrazine binding (see also Fig. 6) at a site with no direct interaction with a ligand of the iron. The latter observation implies either that the interaction between the Fe ligands and the Q_B plastoquinone (displaced by atrazine) is equivalent to whatever displaces it or that the quinone is absent from the Q_B binding site. The latter is supported by the slow millisecond kinetics for Q_A^- to Q_B electron transfer in the BBY membranes (Fig. 1 of Ref. 24) arguing for an electron transfer, rate-limited by plastoquinone diffusion into an initially empty Q_B binding site.

We have argued for homology of inhibitor binding sites in bacterial reaction centers containing Fe(II) and PS II centers containing Fe(III), despite the difference in the iron oxidation state and the small differences in the iron environment: slightly different quadrupole splittings in the Fe(II) Mössbauer spectra [36] and the inability to oxidize the iron in *Rb. sphaeroides* reaction centers (unpublished results). The binding sites of the inhibitors are, however, most likely the same in all cases, requiring highly specific interactions with conserved regions of the reaction center complex.

Like the inhibitor studied here, we saw in the accompanying paper [24] that exogenous quinones, which bind to the reaction center, are also capable of distorting the Fe(III) spectrum. Of the quinones examined in Ref. 24, two of them (*p*-BQ and 2,5-diCl-*p*-BQ) showed additional features at $g = 6.8$. Each of the four inhibitors studied here, as well as the quinones of the preceding paper [24], affect the iron environment to an extent which depends on their chemical properties, their proximity to iron ligands and on the pH. The Fe(III) EPR spectrum is thus a new and sensitive detector of the nature of the molecules binding to the Q_B pocket of their pK values and of the contact points at which these molecules interact with the protein.

Wraight [25] has shown that oxidation of Q_{400}, which we now know to be the acceptor side Fe(II), results in a 300-fold lowered binding affinity for DCMU, in spinach chloroplasts, upon oxidation of the iron at pH 7.5. This result is in approximate agreement with the factor of 100 that we observe in BBY preparations at the same pH. Also consistent is the 10–15-fold lowered affinity for *o*-phenanthroline found here at pH 7 and the factor of 5 reported in Ref. 25. Wraight saw no difference in the dissociation constant for atrazine binding between Q_{400} and Q_{400}^+ while we see here a factor of approx. 10 at pH 7. There is no obvious reason for this discrepancy other than the biological material used. Renger et al. [30] have, however, observed a K_3/K_2 of about 2 at pH 8 for atrazine in BBY membranes. The qualitatively similar results obtained here for the inhibitor dissociation constants in the Fe(III) and Fe(II) states and those obtained by Wraight [25] for the Q_{400}^+ and Q_{400} states, respectively, further reinforce the identification of Q_{400} with the iron.

The smaller shift in the Fe(III)/Fe(II) midpoint potential with atrazine and *o*-phenanthroline made these the inhibitors of choice for looking for the site of light-induced Fe(II) oxidation by exogenous quinones [24,26]. We show in Fig. 5 that both atrazine and *o*-phenanthroline inhibit light-induced oxidation by phenyl-*p*-BQ to a much greater extent than would be predicted from the increase in the Fe(III)/Fe(II) midpoint potential alone. As these inhibitors bind directly to the Q_B binding site [1–7,18–20,34], we conclude that phenyl-*p*-BQ and the other quinones which show the same effect, likewise bind to the same site. The distortion of the Fe(III) spectrum by *p*-BQ and 2,5-diCl-*p*-BQ (Fig. 5 of Ref. 24) and its disappearance upon addition of atrazine (Fig. 6, this paper) support this argument. At the high concentrations used (approx. 1 mM) the quinones are at least partially bound to the Q_B site prior to illumination at 200 K [24]. Upon warming to 0 °C, electron transfer occurs from Q_A^- to Q_{ex} in the Q_B site, whereupon the semiquinone oxidizes the iron to Fe(III). That this reaction will occur at 240 K [24], where the quinone is unlikely to diffuse, would also argue that there is bound quinone preceding illumination at 200 K. At 2 mM *p*-BQ and phenyl-*p*-BQ, at least 50% of the centers show light-induced oxidation of Fe(II) upon warming to 240 K. At this quinone concentration, therefore, more than half the centers have bound quinone. Maximum oxidation of the Fe(II) undoubtedly requires diffusion of exogenous quinone into empty Q_B sites at higher temperature.

We have shown in Fig. 2 that DCMU, which also binds to the Q_B site, slows access of ferrocyanide to Fe(III). This observation would argue that this tetranionic reductant also acts through the Q_B site. While not directly demonstrated here, it is likely that ferricyanide, which has one charge less, oxidizes the Fe(II) through the same route. Indeed Wraight [25] has shown that the rate of oxidation of Q_{400} by ferricyanide is greatly slowed ($t_{1/2}$ increased from 2–3 min to more than 50 min by the addition of 10 μM DCMU).

We have shown in this and in the preceding paper that an electron can pass from Q_A^- to Fe(III) and from Fe(II) to a semiquinone in the Q_B site. In both cases the electron presumably passes through the highly polarizable histidine imidazoles. While we show that, under certain circumstances, the iron is indeed a pathway for electron transfer between the quinones, we do not resolve the question of iron involvement in physiological Q_A^- to Q_B electron transfer.

It is unlikely, from what we know of photosynthetic bacterial reaction centers, that the metal changes its oxidation state from M(II) to M(III) during the normal course of electron transfer from Q_A^- to Q_B, particularly as a replacement by Zn(II) with its full 3d orbitals does not alter the rate [37]. The metal could facilitate vibronic coupling [38,39], channel the wave function for the Q_A to Q_B electron transfer or simply coordinate the histidine imidazoles which are themselves the channel for electron transfer. In the latter case, whether only the linear histidines or all four [18] are implicated, could be determined by histidine replacement using recombinant DNA techniques.

It is of course possible that the iron plays no role at all in Q_A to Q_B electron transfer and that its presence and conservation in reaction centers arises from a different function entirely. Possible other roles for the iron are a coordination site for assisting assembly of the reaction center subunits or as an oxidase possibly involved in plastoquinone pool oxidation.

Acknowledgements

The authors would like to thank Drs. A. William Rutherford and Jean-Luc Zimmermann for their open and generous discussion of results of mutual interest during the course of this project and their making available a preprint of their work. We would also like to thank Dr. Shigeru Itoh, who made available to us a preprint of his recent work, during the preparation of this manuscript. We are grateful to Drs. Klaus Brettel, Antony Crofts, G. Charles Dismukes, Jérôme Lavergne, Peter Rich, Stenbjørn Styring, Jean-Pierre Tuchagues and Bruno Velthuys for their valuable discussions and suggestions. We gratefully acknowledge, as well, the support of the CNRS contract no. 980029 and of an EMBO travel grant.

References

1 Okamura, M.Y., Isaacson, R.A. and Feher, G. (1975) Proc. Natl. Acad. Sci. USA 72, 3491–3495
2 Velthuys, B.R. (1981) FEBS Lett. 126, 277–281
3 Wraight, C.A. (1981) Isr. J. Chem. 21, 348–354
4 Lavergne, J. (1982) Biochim. Biophys. Acta 682, 345–353
5 Jursinic, P. and Stemler, A. (1983) Plant Physiol. 73, 703–708
6 Diner, B.A., Schenck, C.C. and De Vitry, C. (1984) Biochim. Biophys. Acta 766, 9–20
7 Crofts, A.R. and Wraight, C.A. (1983) Biochim. Biophys. Acta 726, 149–185
8 Oettmeier, W., Masson, K. and Johanningmeier, U. (1980) FEBS Lett. 118, 267–270
9 Pfister, K., Steinbeck, K., Gardner, G. and Arntzen, C.J. (1981) Proc. Natl. Acad. Sci. USA 78, 981–985
10 Johanningmeier, U., Neumann, E. and Oettmeier, W. (1983) J. Bioenerg. Biomemb. 15, 43–66
11 De Vitry, C. and Diner, B.A. (1984) FEBS Lett. 167, 327–331
12 Gilbert, C.W., Williams, J.G.K., Williams, K.A.L. and Arntzen, C.J. (1985) in Molecular Biology of the Photosynthetic Apparatus (Steinbeck, K., Bonitz, S., Arntzen, C.J. and Bogorad, L., eds.), pp. 67–71, Cold Spring Harbor Laboratory
13 Wolber, P.K. and Steinbeck, K.E. (1984) Z. Naturforsch. 39c, 425–429
14 Hirschberg, J. and McIntosh, L. (1983) Science 222, 1346
15 Erickson, J.M., Rahire, M., Rochaix, J.D. and Mets, L. (1985) Science 228, 204–207
16 Pakrasi, H. and Arntzen, C.J. (1987) Biochemistry of Plants, Vol. 14 (Hatch, M.D. and Boardman, N.K., eds.), Academic Press, New York, in the press
17 Schenck, C.C., Sistrom, W.R., Bunzow, J.R., Rambousek, E.L. and Capaldi, R.A. (1986) Biochemistry, in the press
18 Michel, H., Epp, O. and Deisenhofer, J. (1986) EMBO J. 5, 2445–2451
19 Chang, C.H., Tiede, D., Tang, J., Smith, U., Norris, J. and Schiffer, M. (1986) FEBS Lett. 205, 82–86
20 Allen, J.P., Feher, G., Yeates, T.O., Komiya, H. and Rees, D.C. (1987) Biophys. J. 51, 377a

21 Petrouleas, V. and Diner, B.A. (1986) Biochim. Biophys. Acta 849, 264–275
22 Ikegami, I. and Katoh, S. (1973) Plant Cell Physiol. 14, 824–836
23 Bowes, J.M., Crofts, A.R. and Itoh, S. (1979) Biochim. Biophys. Acta 537, 320–335
24 Petrouleas, V. and Diner, B.A. (1987) Biochim. Biophys. Acta 893, 126–137
25 Wraight, C.A. (1985) Biochim. Biophys. Acta 809, 320–330
26 Zimmermann, J.L. and Rutherford, A.W. (1986) Biochim. Biophys. Acta 851, 416–423
27 Berthold, D.A., Babcock, G.T. and Yocum, C.F. (1981) FEBS Lett. 134, 231–234
28 Tischer, W. and Strotmann, H. (1977) Biochim. Biophys. Acta 460, 113–125
29 Vermaas, W.F.J., Dohnt, G. and Renger, G. (1984) Biochim. Biophys. Acta 765, 74–83
30 Renger, G., Hagemann, R. and Fromme, R. (1986) FEBS Lett. 203, 210–214
31 Stein, R.R., Castellvi, A.L., Bogacz, J.P. and Wraight, C.A. (1984) J. Cell. Biochem. 24, 243–259
32 Vermaas, W.F.J., Renger, G. and Arntzen, C.J. (1984) Z. Naturforsch. 39c, 368–373
33 Deisenhofer, J., Epp, O., Miki, K., Huber, R. and Michel, H. (1985) Nature 318, 618–624
34 Trebst, A. (1986) Z. Naturforsch. 41c, 240–245
35 Itoh, S., Tang, X.S. and Satoh, K. (1986) FEBS Lett. 205, 275–281
36 Petrouleas, V. and Diner, B.A. (1982) FEBS Lett. 147, 111–114
37 Debus, R.J., Feher, G. and Okamura, M.Y. (1986) Biochem. 25, 2276–2287
38 Holton, D., Kirmaier, C., Debus, R.J., Okamura, M.Y. and Feher, G. (1986) Biophys. J. 49, 585a
39 Devault, D. (1986) Photosynthesis Res. 10, 125–136